are not significantly different from those of the first method, so that, on the whole, it is probably preferable to use this method.

The third method is simpler than the other two, but it occasionally misclassifies points, especially when the mapping frequency is calculated over the whole image and is then applied locally at each point. It would be more expensive to compute local frequency mappings (say on regions whose sizes are proportional to the quadtree leaf sizes) but this would undoubtedly lead to better results.

IV. Conclusion

This correspondence has presented three methods of smoothing images using variable numbers of picture points to calculate the smoothing function. While all three methods give good results, the methods using quadtrees are attractive because of the information the quadtree provides about the homogeneity of the regions in the image and about the sizes of neighborhoods that are appropriate at different places in the image.

References

[1] R. C. Gonzalez and B. A. Fittes, "Gray-level transformations for interactive image enhancement," *Mechanism Machine Theory*, vol. 12, pp. 111–122, 1977.

[2] D. J. Ketcham, R. W. Lowe, and J. W. Weber, "Image Enhancement Techniques for Cockpit Displays," Display Systems Laboratory, Hughes Aircraft Co., Culver City, CA., TR-P74-530R, 1974.

[3] D. Milgram, "Region extraction using convergent evidence," *Computer Graphics, Image Processing*, vol. 11, pp. 1–13, 1979.

[4] S. Peleg, "Iterative histogram modification, 2," *IEEE Trans. Syst., Man, Cybern.*, vol. SMC-8, no. 7, pp. 555–556, 1978.

[5] S. Ranade, A. Rosenfeld, and J. M. S. Prewitt, "Use of quadtrees for image segmentation," Computer Sci. Center, Univ. of Maryland, TR-878, College Park, MD.

[6] A. Rosenfeld and A. C. Kak, *Digital Picture Processing.* New York: Academic, 1976.

[7] A. Rosenfeld and L. S. Davis, "Iterative histogram modification," *IEEE Trans. Syst., Man, Cybern.*, vol. SMC-8, no. 4, pp. 300–302, 1978.

Image Enhancement by Local Histogram Stretching

ERHAN ALPARSLAN AND FUAT INCE, MEMBER, IEEE

***Abstract*—An image enhancement algorithm that makes use of local histogram stretching is introduced. This algorithm yields considerable improvements in human observation of details in an image, compared to straightforward histogram equalization and a number of other enhancement techniques. The algorithm is especially suitable for producing hard copies of images on electrostatic plotters with limited gray levels, as shown in applications to the Girl's image and a Landsat image.**

I. Introduction

Most imaging devices such as photoscanners, digital color film scanners, and multispectral scanners can measure and differentiate up to 256 gray levels [1]. This quantity is much larger than the six gray levels differentiated by the eye on a black and white (BW) plot of our Versatec electrostatic plotter. For this reason much detail in a digital image may be lost when an electrostatic plotter is used as the output medium.

One solution to this problem, which is indeed a partial solution, is to map the 256 gray levels in the digital image to the six gray levels obtainable on the output medium by histogram equalization of the whole image. This process achieves maximum overall contrast and increases the general quality of the image. However, details coming from small brightness differences in the original image are still lost.

In order to enhance those details many techniques have been proposed, developed, and used. The computational disadvantages with respect to time, memory, and permissible size of the image, which are inherent in using the transform domain approach, have led to the development of many signal domain techniques as described by Rosenfeld [2], Hummel [3], and others [4]–[7].

This correspondence describes another signal domain enhancement technique, which modifies the value of a pixel using local context information. It is especially suitable for preprocessing of a BW image before plotting it with a limited number of gray levels. Small local differences are accentuated, thus making some edges and lines, which would otherwise be lost, quite visible. This method is different from the local histogram modifications of Himmel [3] because only the brightest and the darkest pixels in a neighborhood are used to modify the central pixel.

II. The Image Enhancement Algorithm

Consider an image A, which is divided into $M \times N$ picture elements by an $M \times N$ grid. A is a group of $n = M \times N$ pixels, characterized by their gray levels

$$A = \{a \mid a_d \leqslant a \leqslant a_b\} \tag{1}$$

where a_d and a_b, respectively, denote the darkest and brightest pixels of the image.

Let $P(a)$ denote the population of a, i.e., the number of pixels, having gray level a. Let m be the number of gray levels obtainable on the output device. Typically $a_b - a_d \gg m$. Then A can be divided into m equipopulated subgroups R_i as follows.

$$A = \bigcup^{m} R_i$$

where

$$R_i = \left\{ a \mid a_d^i \leqslant a \leqslant a_b^i, \ \sum_{j=d}^{b} c_j \cdot P\left(a_j^i\right) = n/m \right\} \tag{2}$$

and a_d^i and a_b^i, respectively, are the gray levels of the darkest and brightest pixels of subgroup R_i.

c_j are the coefficients of the pixel populations, such that the number of pixels in each subgroup R_i are equal. $c_j = 1$ for $d \leqslant j \leqslant b$. But $0 \leqslant c_j \leqslant 1$ at the borders of the subgroups, i.e., when $j = d$ or b.

Elements of each R_i are represented by the gray level i, $1 \leqslant i \leqslant m$, on the output device that has the disadvantages pointed out in Section I. Now, an image enhancement procedure is introduced as follows.

Let a_c be the central pixel of any neighborhood in A. a_c and its neighbors form a subgroup U in A, whose elements are characterized by their gray levels.

$$U = \{a \mid a_d^u < a < a_b^u\}, \qquad U \subseteq A \tag{3}$$

where a_d^u and a_b^u are the gray levels of the darkest and brightest pixels in U, respectively.

The gray level of the pixel a_c is modified with respect to its relative brightness within the window U as follows: a_c is stretched to a testing interval $(1, g)$, g being a positive integer, $g \geqslant m$. The stretched value of a_c, a_c^s is given by

$$a_c^s = \begin{cases} \max\left(1, \dfrac{a_c - a_d^u}{a_b^u - a_d^u} * g\right), & \text{for } a_d^u \neq a_b^u \\ \left\lfloor \dfrac{g+1}{2} \right\rfloor, & \text{for } a_d^u = a_b^u \end{cases} \tag{4}$$

Manuscript received June 18, 1980; revised February 13, 1981.

The authors are with The Scientific and Technical Research Council of Turkey, Marmara Scientific and Industrial Research Institute, P.O. Box 141, Kadikoy, Istanbul, Turkey.

0018-9472/81/0500-0376$00.75

(a)

(b)

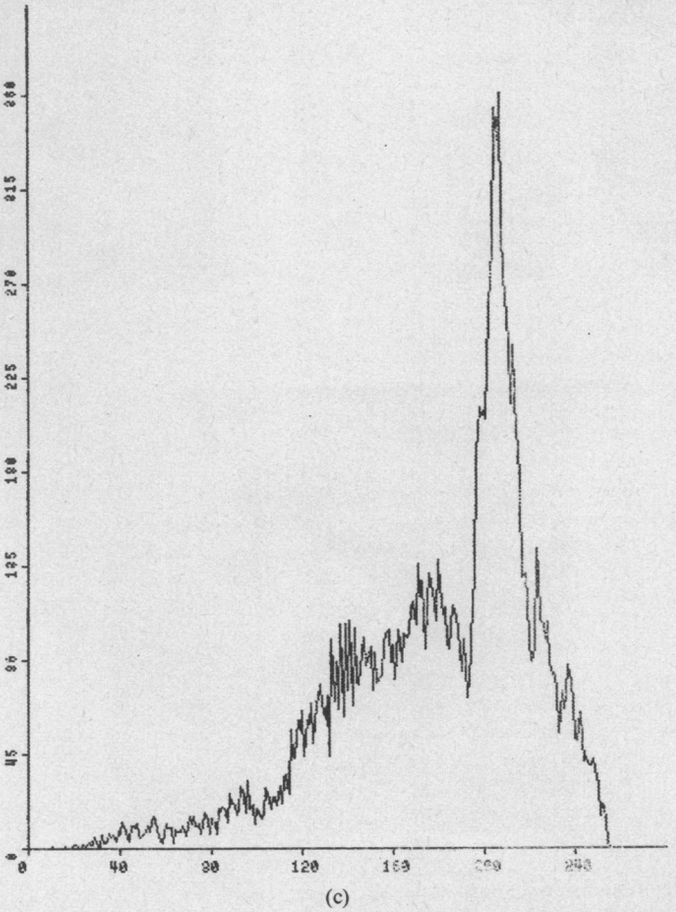

(c)

Fig. 1. (a) Original Girl image. (b) Histogram equalized Girl image. (c) Respective histogram.

(a)

(b)

(c)

(d)

(e)

Fig. 2. Enhancement of Fig. 1(a) with (a) $g=12$, $l=6$, $\#=8$. (b) $g=20$, $l=6$, $\#=8$. (c) $g=12$, $l=6$, $\#=24$. (d) $g=12$, $\#=8$, $W=10$. (e) $g=12$, $\#=8$, $W=4$.

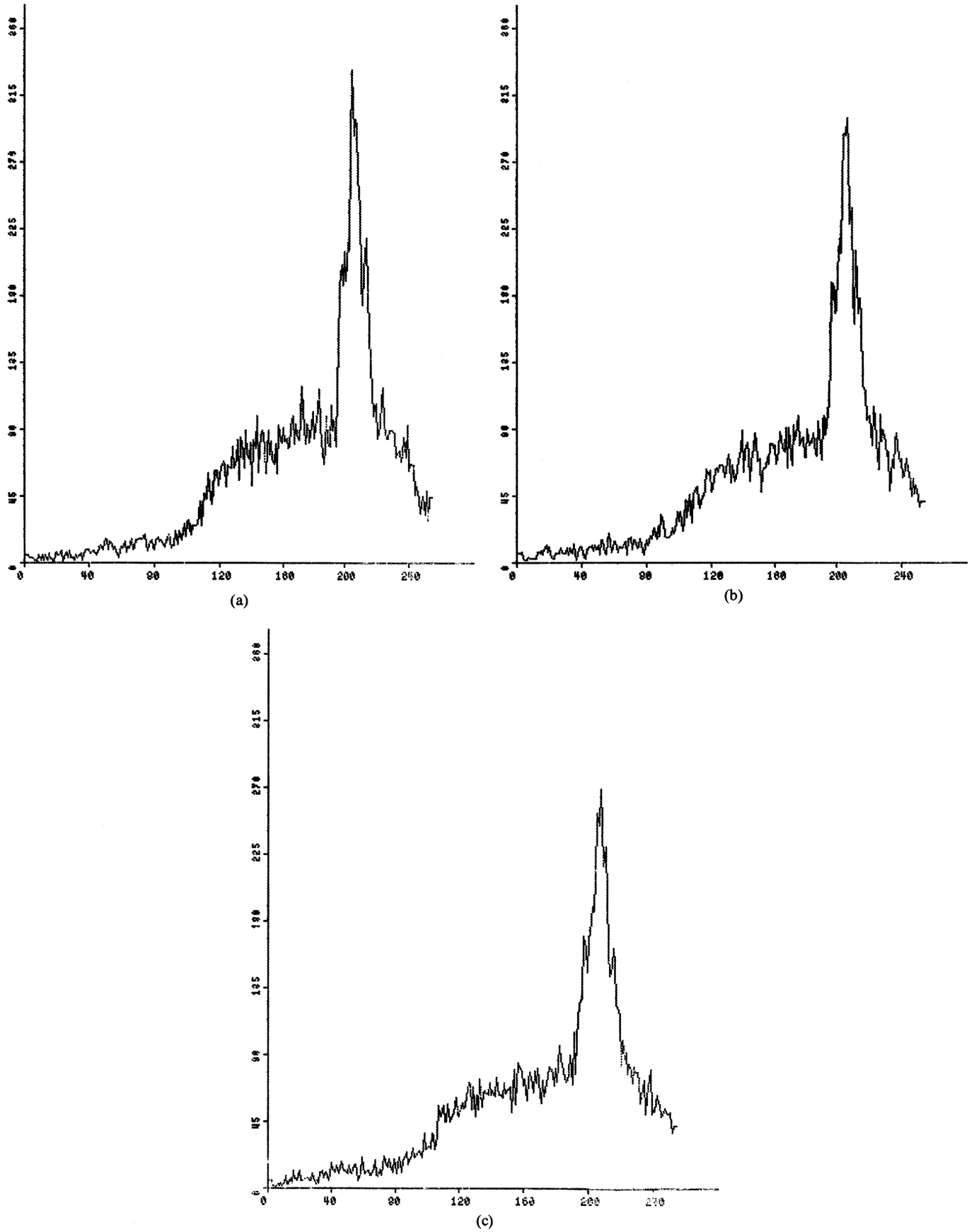

Fig. 3. Respective histograms of Fig. 2.

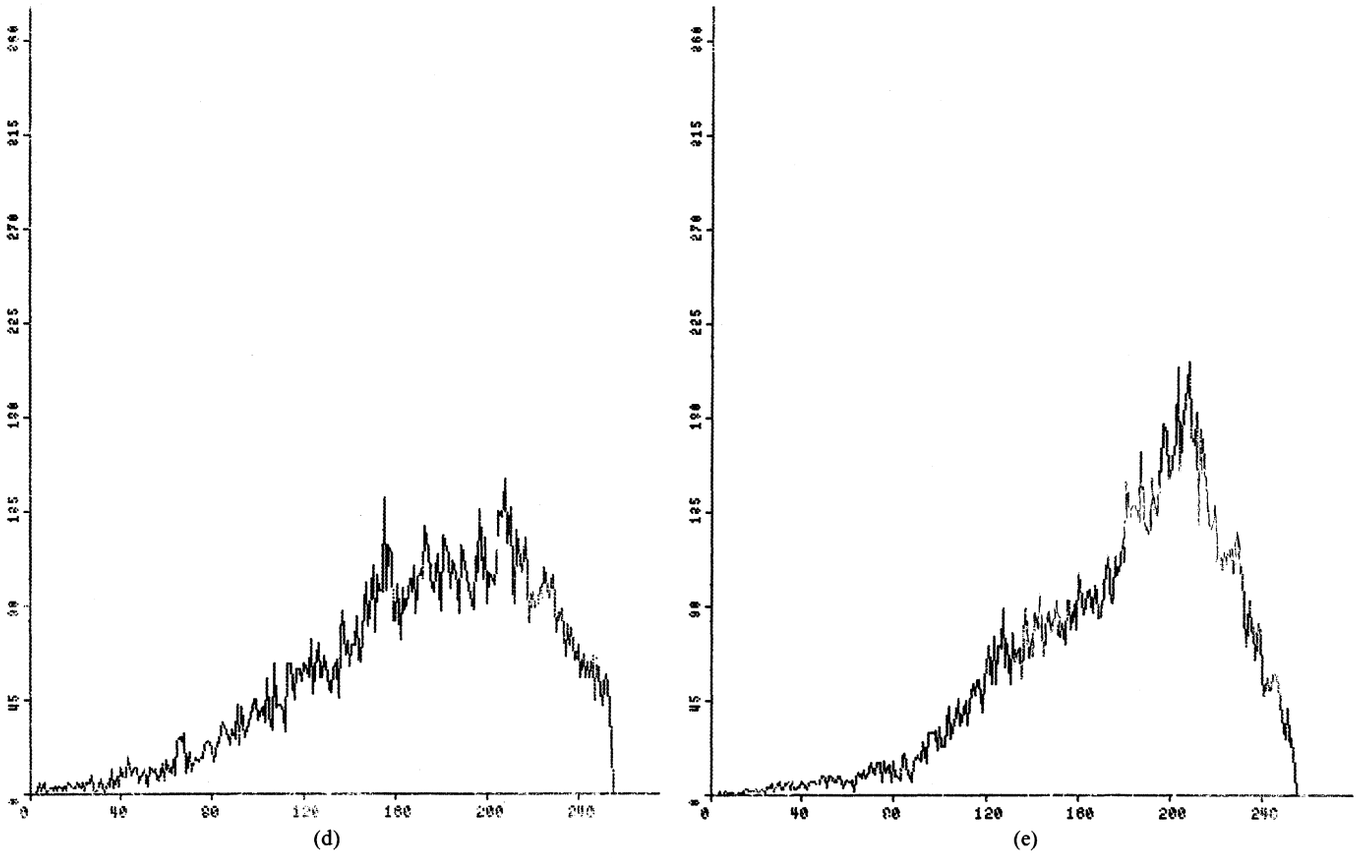

(d) (e)

Fig. 3. *Continued.*

where $\lfloor \cdot \rfloor$ ($\lceil \cdot \rceil$) is the floor (ceiling) operator, which is defined as the first integer value below (above) its argument.

If a_c falls to the low (high) extreme of the interval $(1, g)$, it is a locally dark (bright) spot and it will be punished (rewarded) by a decrease (an increase) in its gray level. The amount of punishment (reward) will be measured by both the position of a_c in the interval $(1, g)$, which determines the value of a function $f(\cdot)$, and the gray level variations inside the window U $(a_b^u - a_d^u)$, which determines a parameter W in calculation of the final value of a_c, a_c^f:

$$a_c^f = a_c + f(a_c^s) * W \tag{5}$$

where $f(\cdot)$ and W are given by

$$f(a_c^s) = \begin{cases} a_c^s - \left\lfloor \dfrac{g+1}{2} \right\rfloor, & \text{if } a_c^s \in \left(1, \left\lfloor \dfrac{g+1}{2} \right\rfloor\right) \\ a_c^s - \left\lceil \dfrac{g+1}{2} \right\rceil, & \text{otherwise} \end{cases} \tag{6}$$

$$W = \frac{a_b^u - a_d^u}{l}. \tag{7}$$

In (7), l is user adjusted for a desired level of enhancement emphasis. W may also be selected by the user as some positive constant, thus making it independent of local gray level variations. For $W = 0$, the original image remains unchanged. As W increases, lines and edges as well as noise become increasingly emphasized, which is typical of high pass filtering processes.

Consider the following cases with regard to any a_c in R_i:

1) If a_c is a locally bright (dark) spot, then a_c is rewarded (punished) and represented by a brighter (darker) level of (2), because when $a_c \approx a_b^u (a_d^u)$, then $a_c^s \approx g(1)$ by (4) and $f(a_c^s) \approx g/2(-g/2)$ by (6). By (5), $a_c^f = a_c + (-)g/2 * W$ and $a_c^f \in R_{i+(-)k}$ for an adequate W in (7), $k \geq 1$.

2) If a_c has average brightness, then the gray level of a_c is not changed. $a \approx (a_b^u - a_d^u)/2$, then $a_c^s \approx g/2$ by (4) and $f(a_c^s) \approx 0$ by (6). By (5) $a_c^f \approx a_c$ and $a_c^f \in R_i$.

3) If a_c is neither too dark nor too bright, then a gray level change occurs, only if both $f(\cdot)$ and W have adequate values.

III. Results

The image enhancement algorithm was programmed on a PDP 11/45 computer and output images were plotted using global histogram stretching of (2), m being equal to six gray levels. The program was mainly written in Fortran; however, the sections which perform the local maximum and minimum computation, stretching, and neighborhood windowing were written in assembler language. The execution time of the program is on the order of 40 s for 128×128 pixel images. The execution time increases as the quantization level g of (4) and the number of neighbors # increase.

Two applications of the algorithm are presented here. The Girl image in Fig. 1(a) is obtained by averaging four pixels to one in the standard 256×256 pixels large Girl image. The Landsat image in Fig. 4(a) depicts a region in eastern Turkey. The histogram equalized versions of these images and the histograms are given in Figs. 1(b), 1(c), 4(b), and 4(c), respectively. All images processed by the image enhancement algorithm, Fig. 2(a)–(f) and Fig. 5(a)–(f) look sharper than the histogram equalized images in Figs. 1(b) and 4(b).

If the quantization level g in (4) increases, then $f(\cdot)$ in (6) increases; the result being a slight increase in details in both the face and the collars of the Girl and in the lower left light area and the wet river bed of the Landsat image. This can be observed in Figs. 2(a) and 5(a) with $g = 12$, $l = 6$ # $= 8$, and Figs. 2(b) and 5(b) with $g = 20$, $l = 6$, # $= 8$. The histograms of these images are given in Figs. 3(a), 6(a), 3(b), and 6(b), respectively. A compari-

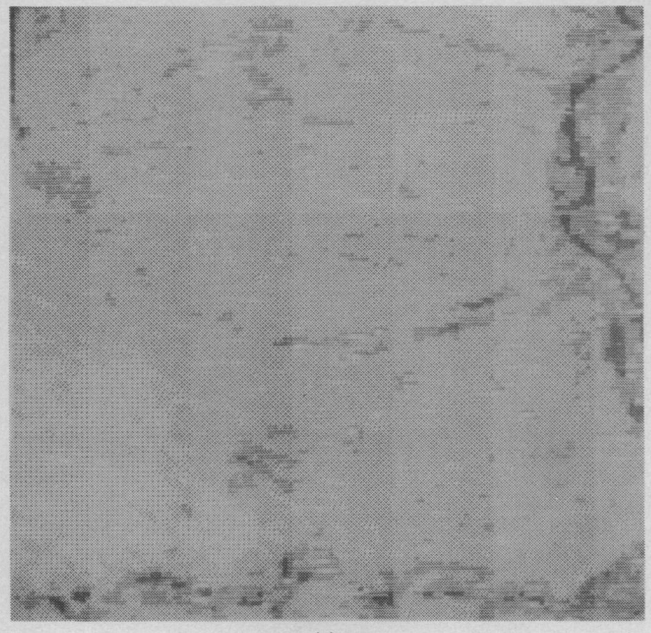

(a)

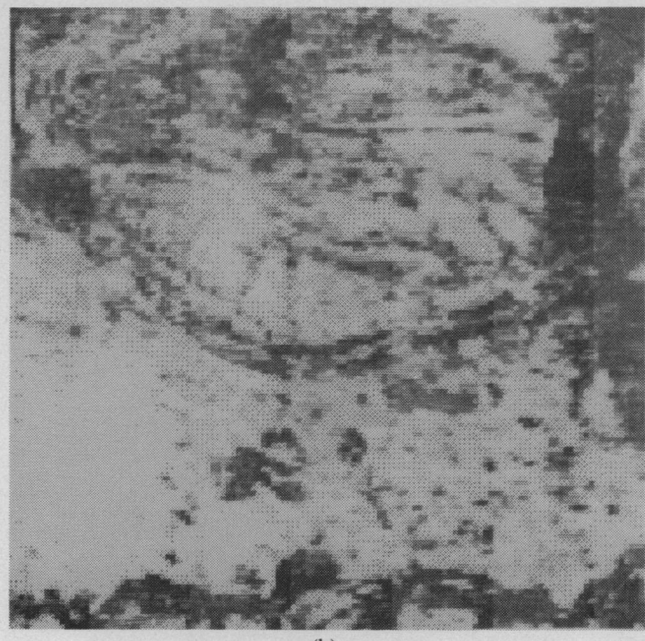

(b)

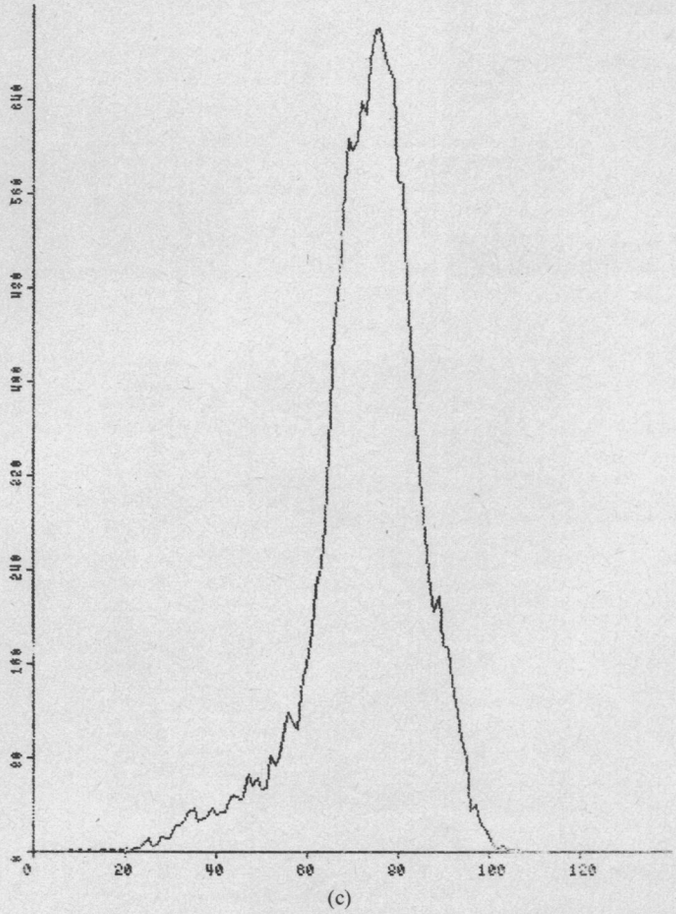

(c)

Fig. 4. (a) Original Landsat image. (b) Histogram equalized Landsat image. (c) Respective histogram.

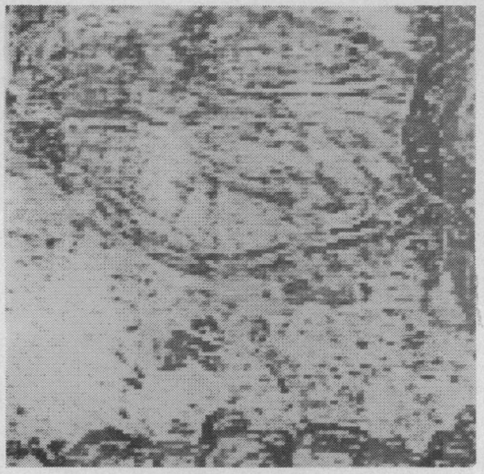

(a)

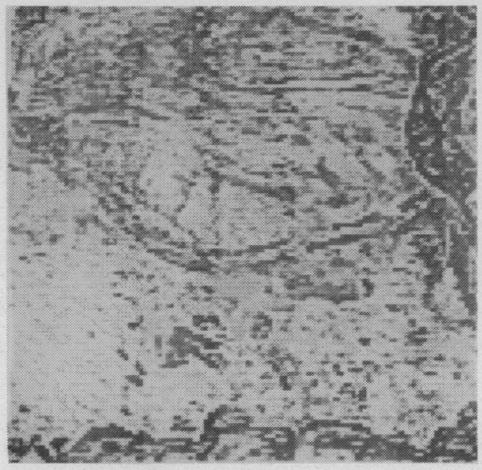

(b)

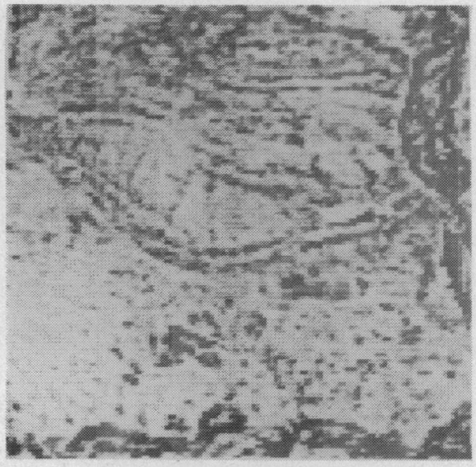

(c)

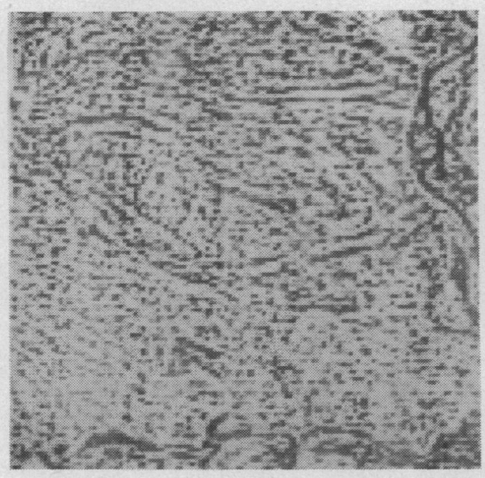

(d)

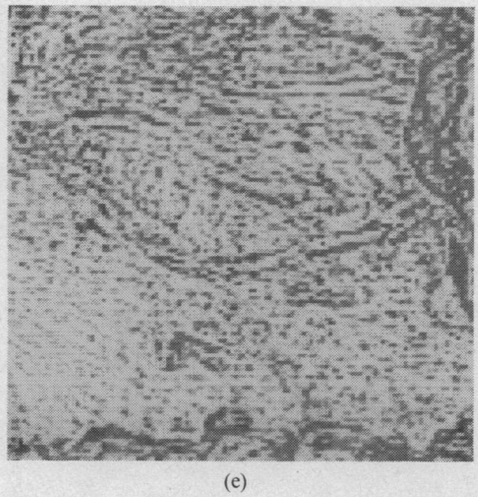

(e)

Fig. 5. Enhancement of Fig. 4(a) with (a) $g = 12$, $l = 6$, $\# = 8$. (b) $g = 20$, $l = 6$, $\# = 8$. (c) $g = 12$, $l = 6$, $\# = 24$. (d) $g = 12$, $\# = 8$, $W = 10$. (e) $g = 12$, $\# = 8$, $W = 4$.

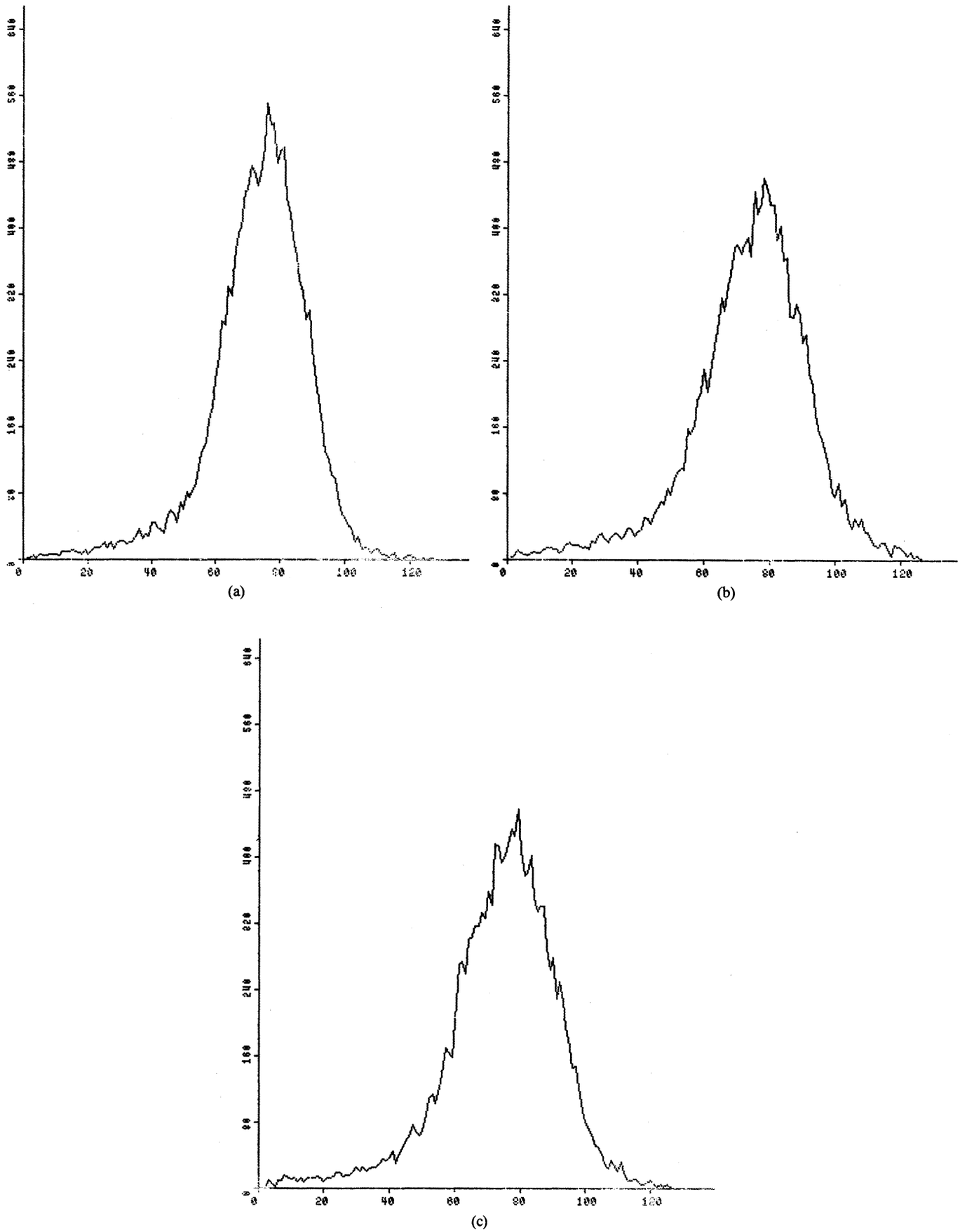

Fig. 6. Respective histograms for Fig. 5.

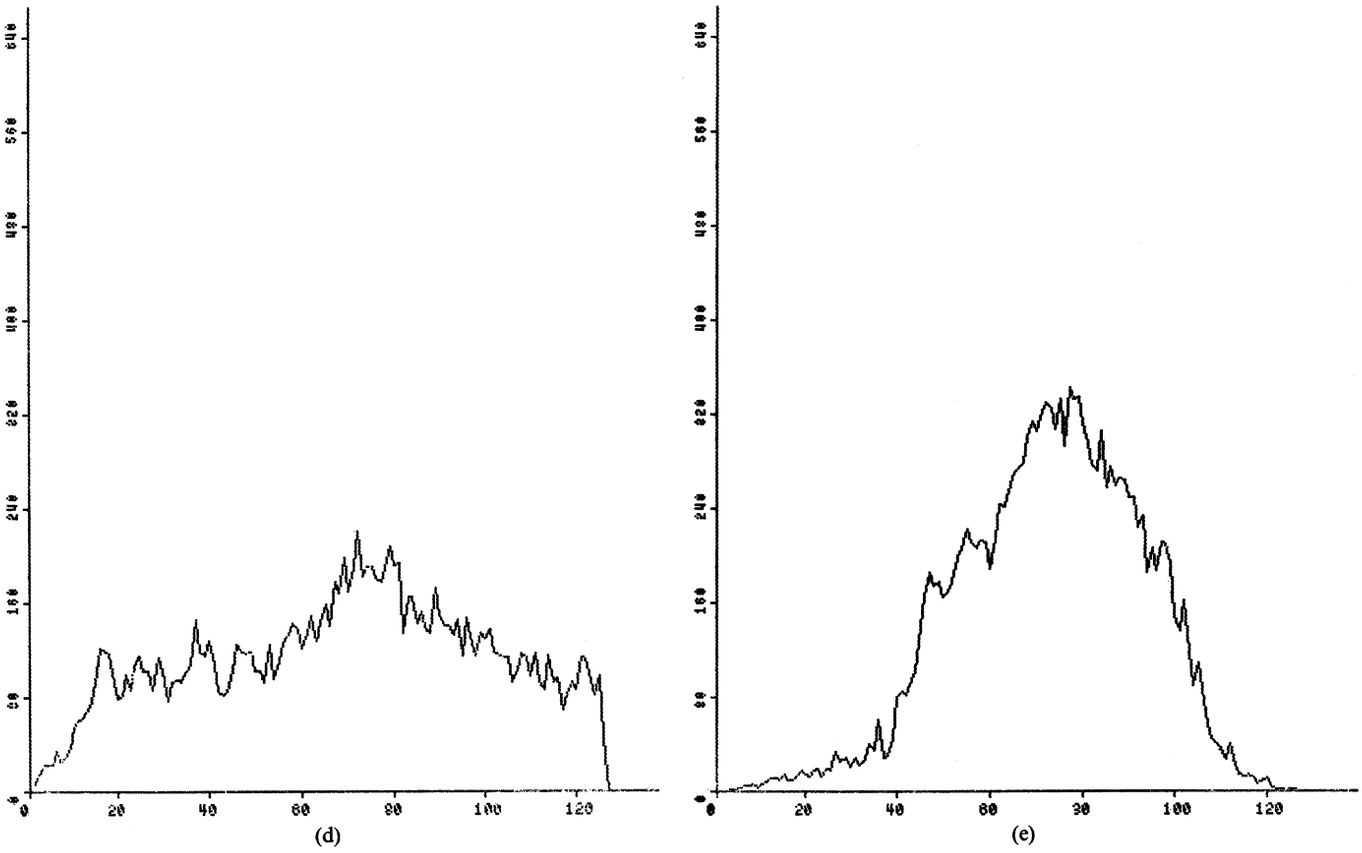

Fig. 6. *Continued.*

son between Figs. 1(c) and 4(c) indicate the following: the peak around gray level 210 in Fig. 1(c) decreases by 8 percent in Fig. 3(a) and by 16 percent in Fig. 3(b). The peak around gray level 75 in Fig. 4(c) decreases by 20 percent in Fig. 6(a) and by 35 percent in Fig. 6(b). The gray levels between 120 and 200 in Fig. 1(c) tend to become more uniformly distributed in Fig. 3(a) and (b). The narrow hill in Fig. 4(c) tend to become wider in Fig. 6(a) and (b), which indicates a stretching in the range of gray level values of the original image.

As more neighbors are taken into consideration, some contours in the images get thicker. This can be seen around the top of the head of the Girl in Fig. 2(c) with $g = 12$, $l = 6$, $\# = 24$, and in the lineaments of the Landsat image of Fig. 5(c) with the same parameters. This effect can be simply explained by considering the increasing effective range of sharp brightness changes. The histograms of these images, given in Figs. 3(c) and 6(c), respectively, are close to the histograms in Figs. 3(b) and 6(b), which indicate that the gray level changes in the respective images are close to each other. Gray level changes in the former case were primarily due to the choice of a large g; in the latter case, it was due to the increase in the range of bright and dark gray levels.

For a sufficiently large reward (punishment), which does not depend on local gray level variations, one can obtain maximum visible detail in all areas of the image, as observed in the face and the dress of the Girl in Fig. 2(d), with $g = 12$, $W = 10$, $\# = 8$, and in the river bed Landsat image lineaments in Fig. 5(d) with the same parameters. But a considerable amount of noise is also introduced, especially on the left wall in the same Girl image between the lineaments of the same Landsat image. The histograms of these images are respectively given in Figs. 3(d) and 6(d). These histograms no longer preserve their original shapes as given in Figs. 1(c) and 4(c); they almost look flat—the peaks around gray level 210 in Fig. 1(c) and around level 75 in Fig. 4(c) are no longer seen. This is because the gray levels all over the images have been modified by globally fixed rewards (punishments). Noise is reduced by decreasing W to 4 as observed in Figs. 2(e) and 5(e). The respective histograms of Figs. 3(e) and 6(e) look smoother than their originals.

IV. Conclusion

In this correspondence, an image enhancement algorithm is described and applied to two images, namely the Girl image of Fig. 1 and the Landsat image of Fig. 4, which are assumed to be representatives for a broad class of similar images. The image enhancement algorithm tends to equalize all gray levels in an image, as observed from the histograms of the enhanced images. A good choice of parameters g, W, and $\#$, yields images whose histograms preserve the overall shape of the histogram of the unprocessed image, whose gray levels have an almost uniform distribution, and which look sharp in appearance. One can observe that the 8 neighbors, i.e., $\# = 8$ is sufficient for most enhancement purposes, bringing out smaller details with less artifacts. For sufficiently large g, W, and small l, the values of some pixels in the unprocessed image are driven out of the gray level range of the image. These values are truncated at both ends. However, one must be careful in the selection of g, l, or W, so as not to drive more than 2 percent of the pixels out of the gray level range of the unprocessed image in order to prevent clipping and undue emphasis.

The image enhancement algorithm makes use of two rewarding (punishing) schemes, the locally variable rewarding (punishing) scheme and the globally fixed rewarding (punishing) scheme. The former scheme emphasizes only the details in the regions with large gray level variations. Thus so enhanced, these images differ from the unprocessed images only in these regions. The latter scheme ignores local gray level variations and imposes a fixed reward (punishment) to all regions of the image; thus it is more

susceptive to noise. However, this scheme is useful for strong emphasis of the smallest details and brightness changes.

References

[1] R. Schmidt, "The USC image processing institute data base," Univ. Southern California Image Processing Inst., Rep. 780, 1977.
[2] A. Rosenfeld and A. C. Kak, *Digital Picture Processing.* New York: Academic, 1976.
[3] R. A. Hummel, "Image enhancement by histogram transformation," *Comput. Graphics and Image Processing*, vol. 6, pp. 184–195, 1977.
[4] R. C. Gonzalez and B. A. Fittes, "Gray level transformations of interactive image enhancement," *Mech. and Mach. Theory*, vol. 12, pp. 111–122.
[5] E. L. Hall, "Almost uniform distributions for computer image enhancement," *IEEE Trans. Comput.*, vol. C-23, no. 2, pp. 207–208.
[6] L. R. Rabiner and B. Gold, *Theory and Application of Digital Signal Processing.* Englewood Cliffs, NJ: Prentice-Hall, 1975.
[7] W. K. Pratt, *Digital Image Processing.* New York: Wiley, 1978.

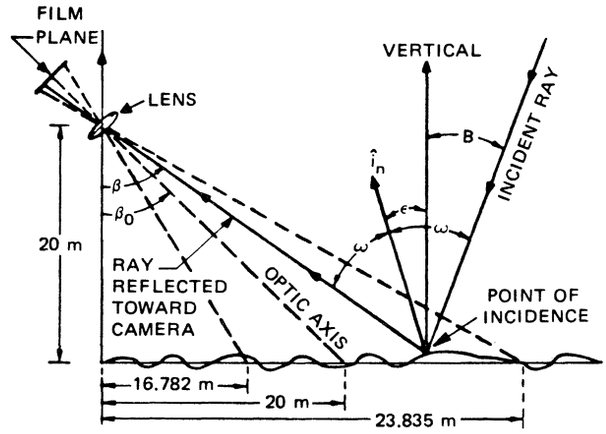

Fig. 1. Experimental geometry and definitions of symbols.

Homomorphic Filtering of Specular Scenes

JOHN S. OSTREM, MEMBER, IEEE

Abstract— **The interpretation and inadequacies of homomorphic filtering as applied to images of specular scenes are discussed.**

In a recent paper, Schreiber [1] commented that while Stockham's homomorphic filtering procedures [2], [3] are useful for improving image quality, they work for reasons other than those originally cited by Stockham. The original interpretation was basically as follows. Image formation can be modeled as the product of reflectance and illumination. The homomorphic filtering procedure of first taking the logarithm separates the effects of reflectance and illumination, thereby allowing image quality to be improved by selectively deemphasizing the effects of uneven scene illumination by linear high-pass filtering (assuming that illumination variations are slow compared with reflectance variations).

This correspondence will show quantitatively that for specular images the preceding interpretation of homomorphic filtering is, in fact, not appropriate. We emphasize specular images because 1) it is straightforward to model specular image formation and therefore to evaluate quantitatively the physical effects of homomorphic filtering, and 2) there are physical images of interest that are essentially specular in nature, such as images of the ocean, to which image processing techniques can be usefully applied.

To understand the effect of homomorphic filtering on images of specular scenes, it is necessary to understand the classical model for specular image formation. The physical basis for specular image formation can best be described in the context of a specific experimental configuration such as the following. A camera is mounted on a platform 20 m above the mean surface level with its optic axis pointed downward at 45° from the vertical. The field-of-view of the camera optics is 10°, so that a scene length of 7.05 m is imaged onto the film plane of the camera.

The solid line in Fig. 1 indicates the path of a light ray originating from the source of illumination (such as diffuse skylight) and reflected off the specular surface into the field-of-view of the camera (indicated by the outer dashed lines). For simplicity, we consider only a two-dimensional configuration in which the incident ray, the normal to the surface at the point of incidence $\hat{i}_n$, and the ray reflected towards the camera are all in the plane of the paper. Hence at the film plane of the camera, a one-dimensional line image will be obtained rather than a full two-dimensional image. Finally, the scene illumination is taken to be unpolarized.

The foregoing restrictions greatly simplify the ensuing discussion yet still allow us to demonstrate the effects of interest. The problem of determining the irradiance distribution at the film plane of a camera for the general three-dimensional case where the illumination is polarized has been treated in detail elsewhere by the author [4]. This paper will draw heavily from [4] for basic concepts and notation.

For the geometry of Fig. 1, the fundamental expression for the image irradiance distribution is [4]

$$H(\beta) = K\eta(\omega)N(B) \tag{1}$$

where β, ω, and B are angles defined in Fig. 1. $H(\beta)$ is the irradiance (W/m^2) at the film plane of the camera; $\eta(\omega)$ is the Fresnel reflectance, which is dimensionless [5]; $N(B)$ is the illumination [$W/(sr \cdot m^2)$], and K is a constant with units [steradians] that contains factors such as the f number of the lens and optical transmittance. Henceforth, we take $K = 1$ to avoid carrying along a simple constant that is unimportant for the purposes of the ensuing discussion.

From simple geometric arguments, it can be shown that $\omega = B - \epsilon$ and $B = \beta - 2\epsilon$ for the configuration of Fig. 1. ϵ is the local slope at the point of incidence, which is positive for slope facets facing towards the camera and negative for those facing away.[1] Substituting $\omega = \beta - \epsilon$, $B = \beta - 2\epsilon$, and $K = 1$ into (1) yields

$$H(\beta) = \eta(\beta - \epsilon)N(\beta - 2\epsilon) \tag{2}$$

or equivalently,

$$\log H(\beta) = \log\eta(\beta - \epsilon) + \log N(\beta - 2\epsilon). \tag{3}$$

It is now possible to see why homomorphic filtering to selectively remove the effects of uneven scene illumination will not, in general, be successful. As stated earlier, the usual assumption or interpretation of homomorphic filtering is that the illumination component of the observed image is slowly varying compared to the reflectance component, so that the effects of the illumination can be selectively deemphasized by high-emphasis linear filtering.[2]

Manuscript received October 10, 1980; revised January 26, 1981.

The author is with the Bioengineering Research Center, SRI International, Menlo Park, CA 94025.

[1] Use of ϵ represents the only notational difference between this correspondence and [4], necessitated because the general three-dimensional problem requires two angles to specify the direction of the normal to the slope at the point of incidence.

[2] More generally, homomorphic filtering would be useful whenever the spectra of $\log\eta(\beta - \epsilon)$ and $\log N(\beta - 2\epsilon)$ are separated, or overlap only partially. However, the usual assumption is that $\log N(\beta - 2\epsilon)$ is slowly varying compared with $\log\eta(\beta - \epsilon)$.

0018-9472/81/0500-0385$00.75